

## Computation of the effect of pH on spur chemistry in water radiolysis at elevated temperatures

Dorota Swiatla-Wojcik

**Abstract.** Diffusion-kinetic model has been employed to calculate the effect of pH and associated ionic strength on the primary yields in the radiolysis of water from ambient temperature to 200°C. Account has been taken of the effect of ionic strength,  $I$ , up to  $0.1 \text{ mol}\cdot\text{dm}^{-3}$  in both acidic and alkaline solutions resulting from the addition of  $\text{H}^+$  and  $\text{OH}^-$ , assuming the counter ions have unit charge. The primary yields are essentially independent of pH for  $I \leq 10^{-4}$ . Above  $I = 10^{-4} \text{ mol}\cdot\text{dm}^{-3}$  the primary yields of  $e_{\text{aq}}^-$  and  $\text{H}_2$  in acidic solutions decrease whereas the primary yields of the H atom, hydroxyl radical and hydrogen peroxide increase. At  $I > 10^{-3} \text{ mol}\cdot\text{dm}^{-3}$  in alkaline solutions, the OH radical and hydrogen peroxide are partially converted into  $\text{O}^{\cdot-}$  and  $\text{HO}_2^-$ , respectively. Increases in the total yields  $G_{\cdot\text{OH}} + G_{\text{O}^{\cdot-}}$  and  $G_{e_{\text{aq}}^-} + G_{\text{H}\cdot}$  and a decrease in  $G_{\text{H}_2\text{O}_2} + G_{\text{HO}_2}$  have been found with increasing pH. At elevated temperatures the effect of pH is diminished. The temperature effect on the primary yields in acidic and alkaline solutions is nearly the same as in neutral water.

**Key words:** effect of pH • radiolysis of water • elevated temperatures • diffusion-kinetic calculations

### Introduction

A knowledge of the radiation chemical yields of all the primary species:  $e_{\text{aq}}^-$ ,  $\cdot\text{OH}$ ,  $\text{H}\cdot$ ,  $\text{H}_2$  and  $\text{H}_2\text{O}_2$ , in the radiolysis of liquid water at high temperatures is very important for nuclear power engineers. In pressurized (PWR) and boiling (BWR) water nuclear power reactors the water coolant is exposed to a mixed flux of 2 MeV neutrons and  $\gamma$ -rays at ca. 300°C. Radiolysis of the coolant leads to formation of oxidants inducing stress corrosion cracking of in-core components. Of basic interest for nuclear power engineers is to know real concentration of the oxidants and to select conditions at which their formation could be suppressed. For example, hydrogen injection in BWR or addition of  $2 \times 10^{-4} - 4 \times 10^{-4} \text{ M LiOH}$  to the end-shield and calandria vault light water in CANDU reactors are applied to minimize the corrosion of carbon steel pipes [3]. Since direct analysis of reactor water is possible at sampling points far away from the circulation lines computer packages are being developed to model chemistry of the coolant. Apart from the technical data comprising flow rates, temperature profiles and power distribution in core, dose rates, etc., simulation of reactor water requires a knowledge of the radiation chemistry of water at high temperatures and high pressures. Similarly, as under ambient temperature and normal pressure, the radiolysis of water coolant proceeds with formation of transient reactive species which are initially located in a track along the radiation path. The development of a track involves thermalization, transformation and reactions of the transient species. Simultaneous diffusion of the species and consequent expansion of

D. Swiatla-Wojcik  
Institute of Applied Radiation Chemistry,  
Technical University of Łódź,  
116 Żeromskiego Str., 90-924 Łódź, Poland,  
Tel.: +48 42 631 31 09, Fax: +48 42 636 50 08,  
E-mail: swiatlad@p.lodz.pl

Received: 23 October 2007

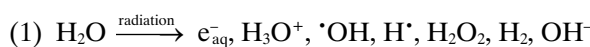
Accepted: 7 February 2008

the track leads to the decay of spatial correlation and homogeneous distribution of the radiolysis products in the bulk medium. The primary yields are the number of the species per absorbed energy, remaining when all the spur/track reactions are complete, i.e. some  $10^{-7}$  s after the energy deposition. Their values are necessary to estimate rate of production of the radiolysis products in the coolant.

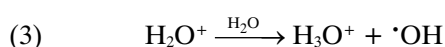
The present work concerns the radiation chemical stage of the low-LET track in water, from about 1 ps, when ionization, dissociation, and thermalization processes result in the initial yields of the radiation generated species, to  $10^{-7}$  s when a decay of the track is over. Low linear energy transfer (LET) radiation, such as  $\gamma$ -rays, hard X-rays or fast electrons, produces a track of isolated spurs of spherical symmetry. Objective is to calculate the effect of pH on the spur chemistry and the resulting primary yields in  $\gamma$ -irradiated water from ambient to elevated temperatures. Such information is required to simulate the operating water chemistry at alkaline conditions or to include effects resulting from the track/spur overlap. Apart from the technological relevance, modelling of the spur chemistry at different pH is interesting from the scientific point of view itself. To our knowledge the effect of pH on the primary yields in water radiolysis has not been studied as a function of temperature. Moreover, the data reported for room temperature and reviewed by Ferradini and Jay-Gerin [5] show controversies for alkaline solutions. In the absence of detailed information on the effect of pH it is important to compute the primary yields of radical and molecular products and to envisage competition between reactions and diffusion of reactive intermediates in the presence of bulk  $H^+/OH^-$  ions. The calculations presented in this paper have been performed for temperatures from ambient to 200°C. Over this range the rate constants for most of the relevant reactions are well established [3].

## Computational method

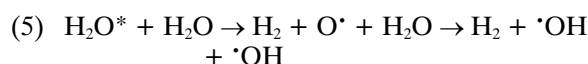
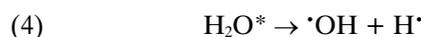
To calculate the effect of pH on the spur chemistry we assume that spurs are embedded in a 'sea' of homogeneously distributed bulk  $H^+$  or  $OH^-$  ions representing acidic or alkaline solutions, respectively. We based on the concept of an average multi-ionization spur and followed the extended diffusion-kinetic approach [6] to model decay of a spur. The applicability of the deterministic modelling for the description of low-LET radiation effects in light and heavy water from ambient to elevated temperatures has been shown [6, 7]. The extended diffusion-kinetic model was described in [6, 7] and only short characteristic of the main features is given below. According to the model an average spur in water comprises:



The initial products result from ionization:



and from dissociative decay of excited molecules:



In liquid water the dissociative fragments are formed in a cage of water molecules and thus can partially recombine. The cage recombination in process (4) leads to a partial reformation of water molecules, whereas in process (5) is responsible for a small prompt yield of hydrogen peroxide, ca.  $0.002 \mu\text{mol}\cdot\text{J}^{-1}$  at room temperature. The probability of partial reformation of water molecules in process (4) decreases from 0.5 at 25°C to 0.07 at 300°C [6]. The  $OH^-$  ions in the spur are products of the dissociative attachment of subexcitation electrons  $e_{\text{sub}}^-$  to the water molecule:



According to the model, the prompt yield of  $OH^-$  and  $H_2$  due to reaction (6) is equal to  $0.026 \mu\text{mol}\cdot\text{J}^{-1}$  [7].

Spatial distribution of the initial products is highly non-homogeneous. Two Gaussian functions of different widths, depending on the length of the thermalization path, have been assumed to describe initial distribution of the species. The broader distribution with a standard deviation of 3.8 nm describes allocation of  $e_{\text{aq}}^-$  and the products of the dissociative attachment of dry electrons in process (6). Distribution of the other species is more compact with a standard deviation of 1.13 nm. Standard deviations of both distributions have been scaled with temperature according to  $(\text{density})^{-1/3}$  [6].

The primary yields have been computed by numerical integration of a set of coupled differential equations describing the temporal and spatial evolution of the concentration  $c_i$  of the reactive species:

$$(7) \quad \frac{\partial c_i}{\partial t} = D_i \nabla^2 c_i - \sum_j k_{ij} \cdot c_i \cdot c_j + \sum_j \sum_k k_{jk} \cdot c_j \cdot c_k$$

where the indices  $i, j$  run over the species listed in Eq. (1). Each equation consists of terms representing diffusion of  $i$ , reactions removing  $i$  and reactions producing  $i$ , respectively. Numerical procedure proposed by Burns and Chance [2] was adopted to deal with the non-Gaussian concentration profiles of reactive intermediates. The reaction space was divided into a number of concentric zones into which the reactants were placed according to the assumed Gaussian distributions and the initial concentrations. The latter have been obtained from the initial yields  $G_i^0$  given in Table 1, assuming the average energy per spur of 83 eV [6]. In each zone reactions take place according to the scheme specified in Table 2. Changes in concentration of the species result from reactions and mass flow between adjoining zones according to the Fick's law of diffusion. The diffusion coefficients of  $e_{\text{aq}}^-$ ,  $H_3O^+$ ,  $\cdot OH$ ,  $H\cdot$ ,  $H_2O_2$ ,  $OH^-$  were taken from Ref. [6]. For  $O\cdot$  and  $HO_2\cdot$  it seemed reasonable to assume  $D_{O\cdot} = D_{F\cdot} = 1.46 \times 10^{-9} \text{ m}^2\cdot\text{s}^{-1}$  [1],  $D_{HO_2\cdot} = D_{O_2\cdot} = 1.75 \times 10^{-9} \text{ m}^2\cdot\text{s}^{-1}$  at room temperature and to follow the temperature dependence for the self diffusion of water [3].

**Table 1.** The initial yields  $G^0$  at room temperature <sup>a)</sup>

Definition	$G^0/(10^{-7} \text{ mol/J})$
Initial yield of excitations, $G_{\text{ex}}^0$	0.78
Initial yield of process (2), $G^0(e_{\text{aq}}^-)$	4.35
Initial yield of process (6), $G^0(\text{H}_2)$	0.26
Initial yield of process (5), $G_2^0(\text{H}_2)$	0.05
Prompt yield of $\text{H}_2$ , $G^0(\text{H}_2) = G_1^0(\text{H}_2) + G_2^0(\text{H}_2)$	0.31
$G^0(\text{H}^+) = G^0(e_{\text{aq}}^-) + G^0(\text{H}_2)$	4.61
Prompt yield of $\text{OH}^-$ , $G^0(\text{OH}^-) = G_1^0(\text{H}_2)$	0.26
Prompt yield of $\text{H}_2\text{O}_2$ , $G^0(\text{H}_2\text{O}_2) = G_2^0(\text{H}_2)/2$	0.025
$G^0(\text{H}^*) = [G_{\text{ex}}^0 - G_2^0(\text{H}_2)](1 - x_{\text{H-OH}})$ <sup>b)</sup>	0.37
$G^0(\cdot\text{OH}) = G^0(\text{H}^+) + G^0(\text{H}^*) + G^0(\text{H}_2)$	5.29

<sup>a)</sup> for details see Ref. [7]. <sup>b)</sup>  $x_{\text{H-OH}}$  is the probability of cage recombination calculated in Ref. [6].

Presence of the bulk  $\text{H}^+/\text{OH}^-$  ions may affect the spur chemistry by reactions with the radiolysis products before they diffuse out of the spur. In the calculations the  $\text{H}_3\text{O}^+$  and  $\text{OH}^-$  ions generated by ionizing radiation were distinguished from the homogeneously distributed bulk ions  $\text{H}^+$ ,  $\text{OH}^-$ . Reactions of the latter have been

**Table 2.** Reaction scheme <sup>a),b)</sup>

Symbols	Reactions
R1	$e_{\text{aq}}^- + \cdot\text{OH} \rightarrow \text{OH}^-$
R2	$e_{\text{aq}}^- + e_{\text{aq}}^- \rightarrow \text{H}_2 + \text{OH}^- + \text{OH}^-$
R3	$e_{\text{aq}}^- + \text{H}^+ \rightarrow \text{H}_2 + \text{OH}^-$
R4	$\cdot\text{OH} + \cdot\text{OH} \rightarrow \text{H}_2\text{O}_2$
R5	$\text{H}^+ + \cdot\text{OH} \rightarrow \text{H}_2\text{O}$
R6	$\text{H}^+ + \text{H}^+ \rightarrow \text{H}_2$
R7	$e_{\text{aq}}^- + \text{H}_2\text{O}_2 \rightarrow \cdot\text{OH} + \text{OH}^-$
R8	$\text{H}^+ + \text{H}_2\text{O} \rightarrow \cdot\text{OH} + \text{H}_2$
R9	$\text{H}^+ + \text{H}_2\text{O}_2 \rightarrow \cdot\text{OH} + \text{H}_2\text{O}$
R10	$\cdot\text{OH} + \text{H}_2\text{O}_2 \rightarrow \text{HO}_2 + \text{H}_2\text{O}$
R11	$\text{O}^{\cdot-} + \cdot\text{OH} \rightarrow \text{HO}_2^-$
R12	$\text{O}^{\cdot-} + e_{\text{aq}}^- \rightarrow \text{OH}^- + \text{OH}^-$
R13	$\text{HO}_2^- + \cdot\text{OH} \rightarrow \text{O}_2^{\cdot-} + \text{H}_2\text{O}$
R14	$\text{HO}_2^- + e_{\text{aq}}^- \rightarrow \text{O}^{\cdot-} + \text{OH}^-$
R15	$\text{H}^+ \rightleftharpoons \text{H}^+ + e_{\text{aq}}^-$
R16	$\text{H}_2\text{O} \rightleftharpoons \text{H}^+ + \text{OH}^-$
R17	$\text{H}^+ + \text{OH}^- \rightleftharpoons e_{\text{aq}}^- + \text{H}_2\text{O}$
R18	$\cdot\text{OH} + \text{OH}^- \rightleftharpoons \text{O}^{\cdot-} + \text{H}_2\text{O}$
R19	$\text{OH}^- + \text{H}_2\text{O}_2 \rightleftharpoons \text{HO}_2^- + \text{H}_2\text{O}$

<sup>a)</sup> reactions which contribution to the spur chemistry in the considered range of temperature and pH exceeds  $10^{-10} \text{ mol/J}$ .

<sup>b)</sup> temperature dependence of the rate constants for reactions R1–R10, R15–R18 as given in Ref. [8], for R11–R14 and R19 as in Ref. [3].

modelled by a first order kinetics with the rate constant equal to the product of the appropriate second-order rate constant and the concentration of bulk  $\text{H}^+/\text{OH}^-$  ions taking into account the effect of the resulting ionic strength. Another effect on the spur chemistry may arise from the ionic atmosphere which facilitates reactions of likely charged reactants and slows down reactions between ions having opposite charges. The correction to the rate constants of reactions between ions was made using the equation [1, 9]:

$$(8) \quad \log(k_{ij}) = \log(k_{ij}^0) + \frac{A \cdot Z_i Z_j \cdot \sqrt{I}}{1 + B \cdot \sqrt{I}}$$

where  $A = 3.65 \cdot 10^6 / (\epsilon \cdot T)^{3/2}$ ;  $B = 150.87 / (\epsilon \cdot T)^{1/2}$ ;  $Z_i$  and  $Z_j$  are the charges on the reactants;  $I$  is the ionic strength;  $T$  is the absolute temperature and  $\epsilon$  is the dielectric constant of the medium, and  $k_{ij}^0$  corresponds to  $I = 0$ .

Integration of the set of differential Eq. (7) have been performed up to  $10^{-7} \text{ s}$  and the concentration of the species have been transformed back into the primary yields.

## Results and discussion

### Ambient temperature

A test of the computational method is presented in Fig. 1. The existing systematic experimental data on pH dependence of the primary yields at room temperature are shown by solid lines [5]. Above pH 11 the experimental results are very scattered. Some reports indicate that primary yields are essentially independent of pH in the range 11–14, but majority agree with an increase in the total yields  $G_{\cdot\text{OH}} + G_{\text{O}^{\cdot-}} + G_{e_{\text{aq}}^-} + G_{\text{H}^*}$ , a decrease of the sum  $G_{\text{H}_2\text{O}_2} + G_{\text{HO}_2^-}$  and almost unaffected  $G_{\text{H}_2}$  compared to neutral solution [5]. The latter observations are consistent with the calculated pH dependence. To show how pH affects spur reactions their cumulative contributions at  $10^{-7} \text{ s}$  have been computed. The cumulative contributions of the main spur reactions are presented

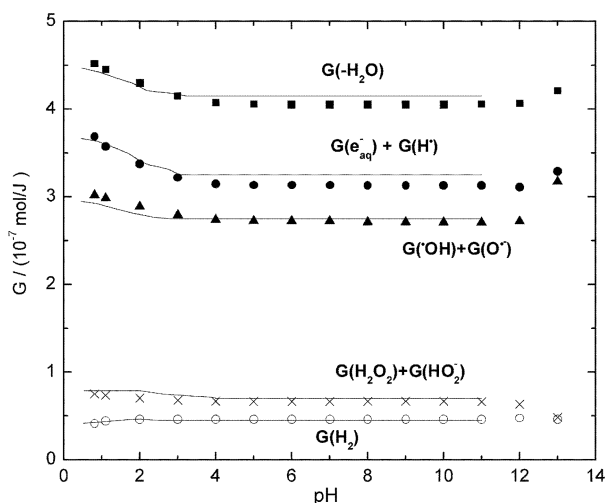


**Fig. 1.** Dependence of the primary radical and molecular yields from the  $\gamma$ -radiolysis of water on pH at room temperature. The experimental data from Ref. [5] are illustrated by solid lines. The calculated yields are represented by points.

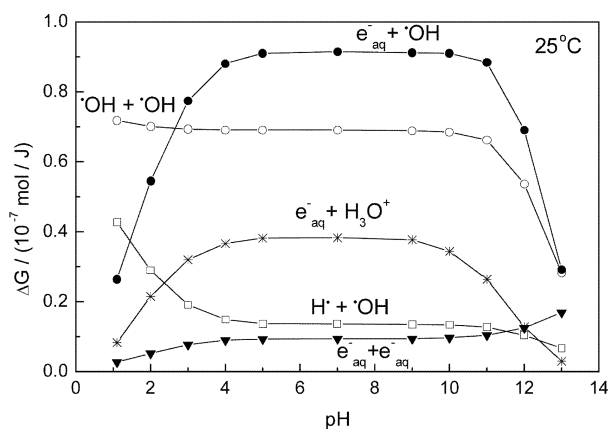


**Fig. 2.** Cumulative contributions of main spur reactions vs. pH computed for 25°C and  $10^{-7}$  s.

as a function of pH in Fig. 2. The lack of pH dependence seen for  $4 < \text{pH} < 11$ . Below pH 4 conversion of  $e_{\text{aq}}^-$  into  $\text{H}^\cdot$  in the reaction with bulk  $\text{H}^+$  starts to compete with the intra-spur reactions. Loss of  $e_{\text{aq}}^-$  suppresses reactions R2 and R3 which are mainly responsible for formation of  $\text{H}_2$  within the spur and results in a decrease of  $G_{\text{H}_2}$  shown in Fig. 1. The decreasing contribution of reaction R1 promotes both diffusive escape of  $\cdot\text{OH}$  radicals and their self-reaction R4. It explains a slight increase of  $G_{\cdot\text{OH}}$  and  $G_{\text{H}_2\text{O}_2}$  at low pH. In alkaline solutions the bulk  $\text{OH}^-$  ions remove the radiation-generated  $\text{H}_3\text{O}^+$  ions and convert  $\text{OH}$  radicals into  $\text{O}^\cdot-$  via forward reaction R18. Consequential protection of  $e_{\text{aq}}^-$  increases the yield  $G_{e_{\text{aq}}^-}$  and the contribution of self-reaction R2. As the latter effect is balanced by the decreasing contribution of reaction R3, not shown in Fig. 2,  $G_{\text{H}_2}$  is almost independent of pH in alkaline solutions.

#### Elevated temperatures

The computed effect of pH on the primary yields of reducing species is shown in Figs. 3–5. The pH dependencies for the oxidizing products are presented in

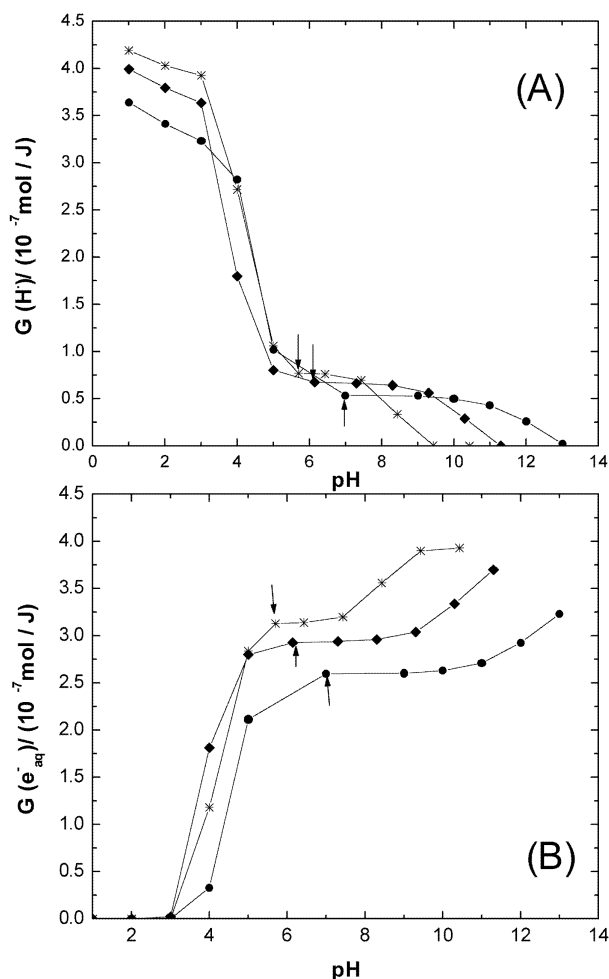


**Fig. 3.** The primary yields of the hydrogen atom (A) and hydrated electron (B) in the  $\gamma$ -radiolysis of water as a function of pH calculated for: 25°C (●), 100°C (◆) and 200°C (\*). Neutral water at each temperature is indicated by an arrow. Points to the left and right hand side of the arrows correspond to the same ionic strength in acidic and alkaline solutions, respectively.

Figs. 6–7. For each temperature under study, neutral water has been indicated by an arrow. Points to the left and right hand side of the arrows correspond to

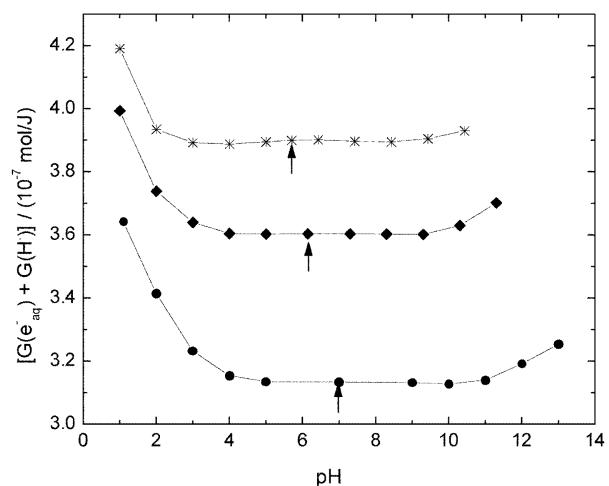


**Fig. 4.** The calculated pH dependence of  $G_{e_{\text{aq}}^-} + G_{\text{H}^\cdot}$  in the  $\gamma$ -radiolysis of water: 25°C (●), 100°C (◆) and 200°C (\*).

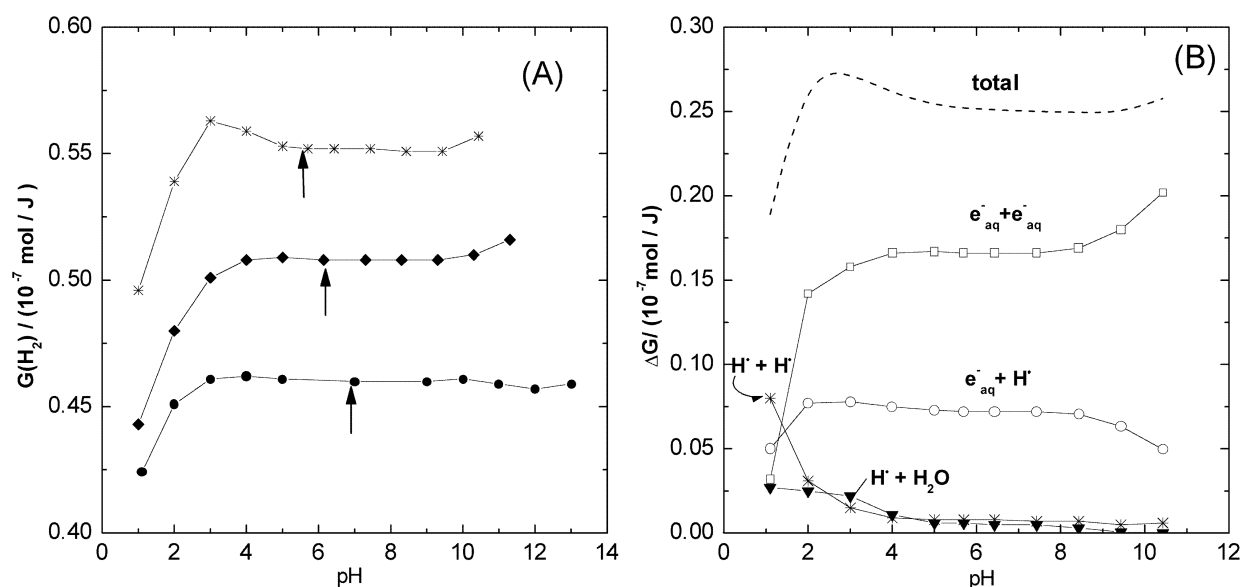


**Fig. 5.** (A) The primary yield of molecular hydrogen in the  $\gamma$ -radiolysis of water as a function of pH calculated for: 25°C (●), 100°C (◆) and 200°C (\*). Neutral water at each temperature is indicated by an arrow. Points to the left and right hand side of the arrows correspond to the same ionic strength in acidic and alkaline solutions, respectively. (B) The cumulative contributions of the intra-spur reactions responsible for the formation of  $\text{H}_2$  at 200°C.

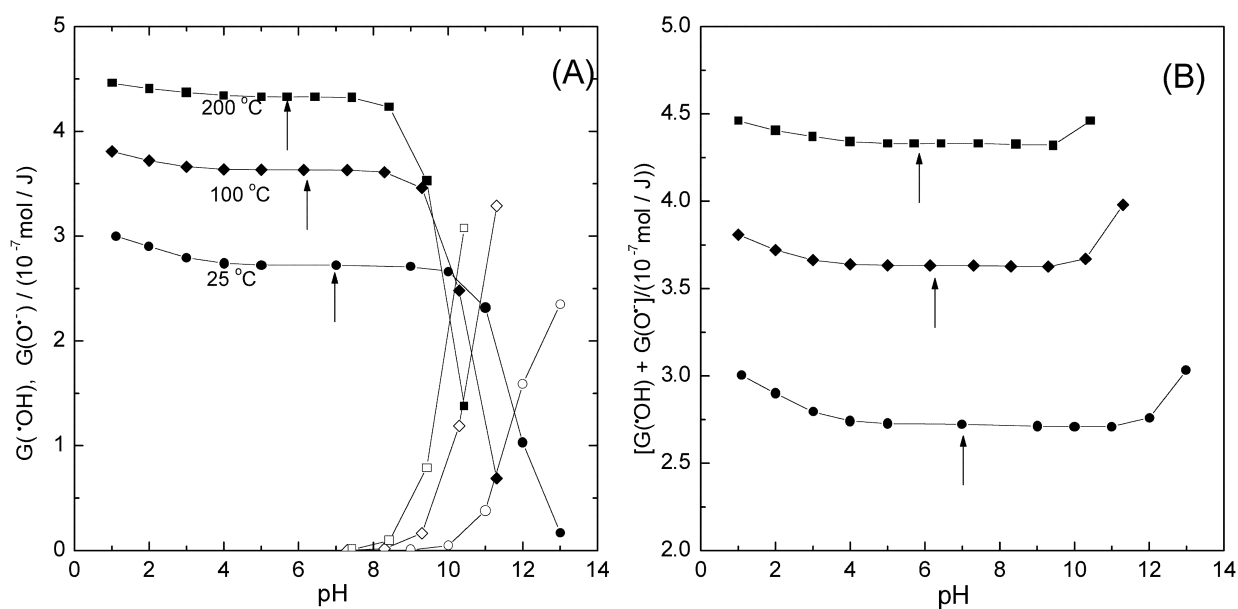


**Fig. 6.** (A) The primary yields of  $\cdot\text{OH}$  (solid symbols) and  $\text{O}^{\cdot-}$  (open symbols) in the  $\gamma$ -radiolysis of water as a function of pH. Neutral water at each temperature is indicated by an arrow. Points to the left and right hand side of the arrows correspond to the same ionic strength in acidic and alkaline solutions, respectively. (B) The effect of pH on  $G_{\cdot\text{OH}} + G_{\text{O}^{\cdot-}}$  calculated for: 25°C (●), 100°C (◆) and 200°C (■).

$I = 10^{-5}, 10^{-4}, 10^{-3}, 10^{-2}, 10^{-1}$  mol·dm $^{-3}$  in acidic and alkaline solutions, respectively. At all studied temperatures,  $G_{\text{H}\cdot}$  in Fig. 3A is increased in acidic and decreased in alkaline solutions. These changes are associated with a respective decrease and increase of  $G_{e_{\text{aq}}^-}$  shown in Fig. 3B.  $G_{\text{H}\cdot}$  and  $G_{e_{\text{aq}}^-}$  are the most affected  $g$  values in acidic solutions. The influence of ionic strength is seen even at  $I = 10^{-5}$  mol·dm $^{-3}$ . Due to conversion of  $e_{\text{aq}}^-$  into  $\text{H}\cdot$  the decrease of  $G_{e_{\text{aq}}^-}$  is partially balanced by increasing  $G_{\text{H}\cdot}$  and, as illustrated in Fig. 4, the sum  $G_{e_{\text{aq}}^-} + G_{\text{H}\cdot}$  is independent of pH for  $I < 10^{-4}$  mol·dm $^{-3}$  at 25 and 100°C. The effect of pH is diminished at 200°C and can be neglected up to  $I = 10^{-3}$  mol·dm $^{-3}$ .

In alkaline solutions  $G_{e_{\text{aq}}^-}$  and  $G_{\text{H}\cdot}$  are less affected by pH. The effect of ionic strength can be neglected for  $I < 10^{-4}$  mol·dm $^{-3}$  (i.e. pH 10 at 25°C). In more alkaline solutions  $G_{e_{\text{aq}}^-}$  increases, whereas  $G_{\text{H}\cdot}$  decreases with increasing pH. The decrease in  $G_{\text{H}\cdot}$  results from the decay of  $\text{H}_3\text{O}^+$  in reaction with bulk  $\text{OH}^-$  and consequent suppression of the backward reaction R15. At 200°C, the increase in  $G_{e_{\text{aq}}^-}$  is almost balanced by the decrease in  $G_{\text{H}\cdot}$  and, as Fig. 4 shows,  $G_{e_{\text{aq}}^-} + G_{\text{H}\cdot}$  is virtually independent of pH.

Spur chemistry of  $e_{\text{aq}}^-$  and  $\text{H}\cdot$  determines the yield of molecular hydrogen. The computed pH dependencies of  $G_{\text{H}_2}$  are shown in Fig. 5A. In Fig. 5B changes of

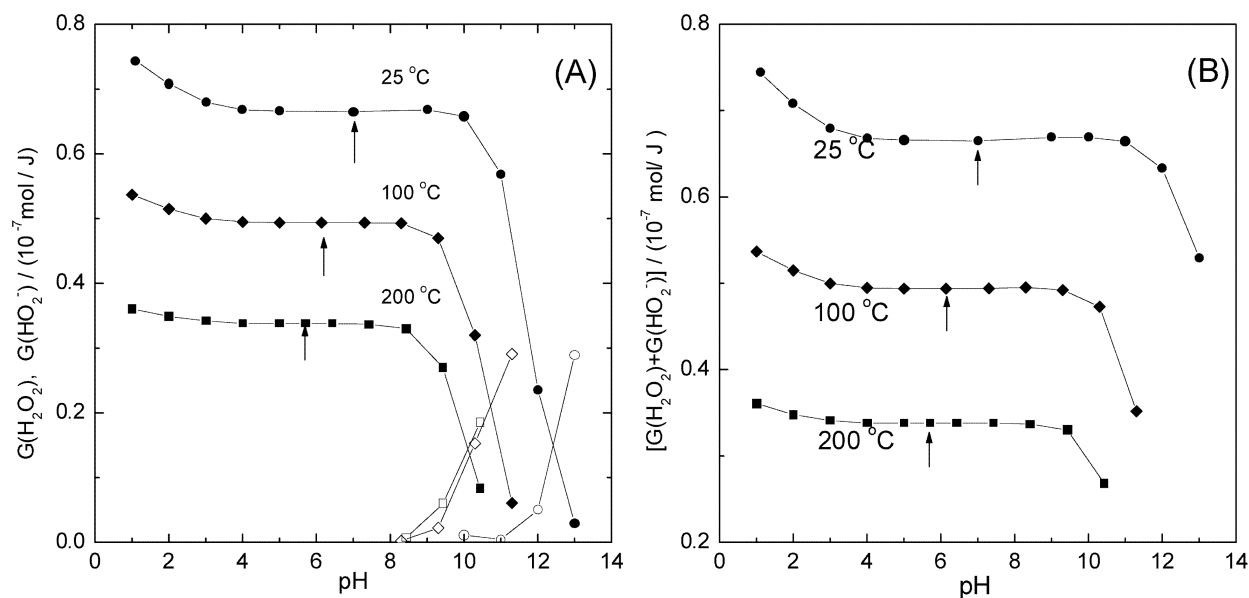


**Fig. 7.** (A) The primary yields of  $\text{H}_2\text{O}_2$  (solid symbols)  $\text{HO}_2^-$  (open symbols) in the  $\gamma$ -radiolysis of water as a function of pH. Neutral water at each temperature is indicated by an arrow. Points to the left and right hand side of the arrows correspond to the same ionic strength in acidic and alkaline solutions, respectively. (B) The effect of pH on  $G_{\text{H}_2\text{O}_2} + G_{\text{HO}_2^-}$  calculated for: 25 °C (●), 100 °C (◆) and 200 °C (■).

the cumulative contributions of spur reactions leading to the formation of  $\text{H}_2$  are illustrated for 200 °C. The main source of  $\text{H}_2$  in neutral and near-neutral water are the intra-spur reactions R2 and R3. In acidic solutions contributions of R2 and R3 are smaller but not meaningless. On the other hand, increasing acidity promotes reaction R6, which cumulative contribution at low pH exceeds that of reactions R2 and R3. As a result, the overall effect of pH in acidic solutions is rather small. At 200 °C, the pH dependence of  $G_{\text{H}_2}$  is not monotonic. The maximum at pH 3 results from reaction R8 whose possible role in the high temperature radiolysis of water has been recently suggested [8]. As shown in Fig. 5B, the cumulative contribution of R8, becomes noticeable for  $I > 10^{-3} \text{ mol}\cdot\text{dm}^{-3}$ . In alkaline solutions no effect of pH is seen up to 200 °C. As can be seen from Fig. 5B, the increase in the cumulative contribution of reaction R2 is balanced by a decreasing contribution of R3.

In acidic solutions influence of pH on  $G_{\text{OH}\cdot}$  and  $G_{\text{H}_2\text{O}_2}$  shown in Figs. 6 and 7, respectively, is rather small and decreases with increasing temperature. In alkaline solutions the effect from the presence of the bulk  $\text{OH}^-$  ions can be neglected for  $[\text{OH}^-] < 10^{-4} \text{ mol}\cdot\text{dm}^{-3}$  at room temperature and for  $[\text{OH}^-] < 10^{-3} \text{ mol}\cdot\text{dm}^{-3}$  at 200 °C. In more concentrated solutions the ionic products of equilibria R18 and R19,  $\text{O}^{\cdot-}$  and  $\text{HO}_2^-$ , respectively, affect the spur kinetics via reactions R11–R14. The most significant are R11 and R12 with the contributions exceeding  $10^{-8} \text{ mol/J}$  at  $I = 0.1 \text{ mol}\cdot\text{dm}^{-3}$ . At all temperatures, the total yield  $G_{\text{OH}\cdot} + G_{\text{O}^{\cdot-}}$  presented in Fig. 5B, increases with pH. The increase of  $G_{\text{OH}\cdot} + G_{\text{O}^{\cdot-}}$  is associated with the decrease of  $G_{\text{H}_2\text{O}_2} + G_{\text{HO}_2^-}$  shown in Fig. 6B.

The effect of temperature on the primary yields in acidic and alkaline solutions is essentially the same as in neutral water [3, 4]. The  $g$  values  $G_{e_{\text{aq}}^-}$ ,  $G_{\text{H}\cdot}$ ,  $G_{e_{\text{aq}}^-} + G_{\text{H}\cdot}$ ,  $G_{\text{H}_2}$ , and  $G_{\text{OH}\cdot}$  shown as functions of pH in Figs. 3–5, and 6, respectively, increase whereas  $G_{\text{H}_2\text{O}_2}$  in Fig. 7 decreases with increasing temperature. Some exceptions can be, however, noticed for  $G_{e_{\text{aq}}^-}$  and  $G_{\text{H}\cdot}$  between

**Table 3.** Comparison of the primary yields calculated for temperature 200 °C and ionic strength  $I = 0.01 \text{ mol}\cdot\text{dm}^{-3}$  using: A – Eq. (8); B – assuming  $k_{ij} = k_{ji}$ . The  $g$  values are expressed in  $10^{-7} \text{ mol/J}$

	Acidic solution		Alkaline solution	
	A	B	A	B
$G_{e_{\text{aq}}^-}$	–	–	3.94	4.04
$G_{\text{H}\cdot}$	4.08	4.18	0.005	0.005
$G_{\text{H}_2}$	0.60	0.56	0.62	0.57
$G_{\text{OH}\cdot}$	4.56	4.57	3.66	3.66
$G_{\text{H}_2\text{O}_2}$	0.36	0.36	0.27	0.28
$G_{\text{O}^{\cdot-}}$	–	–	0.82	0.82
$G_{\text{HO}_2^-}$	–	–	0.06	0.06

$3 < \text{pH} < 5$ . Diffusive escape of the hydrated electrons which are more widely distributed in space, competes with the intra-spur reactions and reaction with the bulk  $\text{H}^+$  ions that converts  $e_{\text{aq}}^-$  into  $\text{H}\cdot$ . Between pH 3 and 5 at 100 °C, diffusive escape of  $e_{\text{aq}}^-$  outweighs its reaction with bulk  $\text{H}^+$ , whereas at 200 °C the decay in reaction with  $\text{H}^+$  prevails resulting in the lower yield of  $e_{\text{aq}}^-$ .

The effect of ionic strength on the spur kinetics increases with temperature, but is not very significant over the studied range. In Table 3, the significance of the ionic strength correction to the rate constants Eq. (8) is illustrated for 200 °C and  $I = 0.01 \text{ mol}\cdot\text{dm}^{-3}$ . Acceleration of the self-reaction R2 results in a lower yield of  $e_{\text{aq}}^-$  in alkaline solution and in a higher yield of  $\text{H}_2$ . On the other hand, the slowing down of the backward reaction R15 slightly decreases  $G_{\text{H}\cdot}$  in acidic solution. There is no effect from the ionic atmosphere on the primary yields of other species.

**Acknowledgment.** Financial support from the Ministry of Science and Higher Education of Poland (grant no. N204 080 32/2232) is gratefully acknowledged.

## References

1. Atkins PW (1998) Physical chemistry. Oxford University Press, Oxford-Melbourne-Tokyo
2. Burns WG, Sims HE, Curtis AR (1984) Radiation chemical diffusion kinetic calculations with prescribed and non-prescribed diffusion. *Radiat Phys Chem* 23:143–180
3. Elliot AJ (1994) Rate constants and *G*-values for the simulation of the radiolysis of light water over the range 0–300°C. AECL Report, AECL-11073, COG-94-167-1
4. Elliot EJ, Chenier MP, Ouellette DC (1993) Temperature dependence of the *g* values for H<sub>2</sub>O and D<sub>2</sub>O with low linear energy transfer radiation. *J Chem Soc Faraday Trans* 89:1193–1197
5. Ferradini C, Jay-Gerin J-P (2000) The effect of pH on water radiolysis: a still open question – a minireview. *Res Chem Intermed* 26;6:549–565
6. Swiatla-Wojcik D, Buxton GV (1995) Modelling of radiation spur processes in water at temperatures up to 300°C. *J Phys Chem* 99:11464–11471
7. Swiatla-Wojcik D, Buxton GV (2000) Diffusion-kinetic modelling of the effect of temperature on the radiation chemistry of heavy water. *Phys Chem Phys* 2:5113–5119
8. Swiatla-Wojcik D, Buxton GV (2005) On the possible role of the reaction  $H + H_2O \rightarrow H_2 + OH$  in the radiolysis of water at high temperatures. *Radiat Phys Chem* 74:210–219
9. Weston RE, Schwarz HA (1972) Chemical kinetics. Prentice-Hall, New Jersey